

SIMULATION AND SELECTION OF DETUMBLING ALGORITHMS FOR A 3U CUBESAT

Vishnu P Katkoo^{a*}, Jivat Neet Kaur^b, Tushar Goyal^c

^a *Department of Chemical Engineering, Birla Institute of Technology and Science (BITS), India,*
vprkatkooi99@gmail.com

^b *Department of Computer Science and Engineering, , Birla Institute of Technology and Science (BITS), India,*
jivatneet@gmail.com

^c *Department of Electrical and Electronics Engineering, , Birla Institute of Technology and Science (BITS), India,*
tushargoyal21@gmail.com

* Corresponding Author

Abstract

As a satellite is deployed from the launch vehicle, it is subjected to high angular rates which need to be dampened in order for the satellite to perform its functions as expected. Simple and robust algorithms, such as BDot, are generally used to provide the required control torque for detumbling the satellite. This paper elucidates the design process for the detumbling algorithm to be implemented on a nanosatellite currently being developed by Team Anant, the Student Satellite Team of BITS Pilani. The process commenced with the selection of hardware to be used on-board the satellite. Magnetometers and Gyroscopes were finalized to be used as sensors. Various commercially available sensor models were then compared based on power and operating conditions. For actuation, a magnetorquer system was designed specifically to the requirements of the team. The system comprised of two magnetorquer rods and a magnetorquer coil aligned in orthogonal directions. The sensors and actuators were then accurately modelled in MATLAB for further testing. The modelling involved some interesting challenges due to the magnetic moment retained by the ferromagnetic core. These challenges, and the ways to overcome them have been also been briefly discussed in the paper. After finalizing the hardware, the team proceeded with implementing various popular control algorithms for detumbling the satellite. The algorithms were first theoretically analysed, and then modelled on MATLAB. The simulations took the space environment around the satellite into consideration for higher accuracy. The algorithms were tested for different initial conditions, using different time-steps and under different power constraints. The algorithms considered and the conclusions derived from these simulations have also been discussed elaborately in this paper. The paper concluded by presenting the finalized detumbling algorithm(s) to be used by Team Anant, and the various conditions devised to ensure efficient use of electrical power. The paper also presents viable alternatives to the finalized algorithm(s), using other hardware components. These alternatives and conditions have also been documented in the paper for a better understanding.

Keywords: ADCS, Satellite Dynamics, Detumbling, Magnetic Actuation

Acronyms/Abbreviations

ADCS - Attitude Determination and Control System

ECI - Earth Centered Inertial

ECEF - Earth Centered Earth Fixed

IGRF - International Geomagnetic Reference Frame

IMU - Inertial Measurement Unit

LEO - Low Earth Orbit

P-POD - Poly-Picosatellite Orbital Deployer

1. Introduction

The Attitude Determination and Control Subsystem, (ADCS) is responsible for ensuring the satellite has the correct attitude in space by providing accurate control to correct any deviation from expected output. Detumbling is essential to stabilize and dampen the high angular rate along all three axes of the satellite after deployment from the Poly-Picosatellite Orbital Deployer (P-POD).

The paper aims to analyse the different detumbling algorithms and select the most efficient control algorithm for a 3U CubeSat in a sun-synchronous, Low Earth Orbit (LEO). The first section describes the detumbling algorithms studied and selected for implementation. The next section discusses the sensors and actuators employed in the satellite to achieve efficient detumbling. Subsequently, a discussion on the

simulation methodology and the various modules implemented to test the algorithms is made. Finally, a comparison of the different algorithms implemented in terms of power consumption, detumbling time and magnetic moment is made.

2. Detumbling Algorithms

Two detumbling algorithms are reviewed within this paper. The first control law requires angular velocity feedback in addition to the ambient magnetic field vector. The second control law, popularly known as the Bdot control law operates exclusively with angular velocity feedback.

2.1 Algorithm 1 – ($\omega \times B$)

In this control law, a magnetic moment is generated perpendicular to the angular velocity and the local magnetic field vector. Angular velocity can be split up into two components - a component which is along the direction of the local magnetic field and a component which is normal to it. The magnetic moment for the control law is calculated as follows [2].

$$m = \frac{k}{\|B\|} (\omega \times B) \quad (1)$$

Here, k is a scalar gain, ω is the angular velocity of the satellite relative to the earth centered inertial (ECI) frame measured in the body frame, and B is the local magnetic field measured in the body frame. This particular selection of magnetic moment ensures that the torque produced is antiparallel to the component of angular velocity normal to the magnetic field. The lack of control along the parallel component of angular velocity is not an issue due to the spatial variation of magnetic field throughout the orbit. The spatial variation of magnetic field is maximized for near polar orbits. Hence, detumbling via magnetic actuation is a viable option for sun-synchronous, LEO orbits.

Feedback for this control law comes from the Inertial Measurement Unit (IMU), as well as the magnetometer.

2.2 Algorithm 2 – Bdot

The Bdot control law calculates magnetic moment using the rate of change of the magnetic field. It utilizes feedback exclusively from the magnetometer. The control law takes the following form [2].

$$m = \frac{-k}{\|B\|} \cdot B^{dot} \quad (2)$$

The rate of change of magnetic field is calculated by using a finite difference method.

$$B_t^{dot} = \frac{B^t - B^{t-1}}{t_{samp}} \quad (3)$$

Here, t_{samp} represents the sampling time. It is noted that this control law is an approximation to the control law described by algorithm 1 [1]. In addition, this control law can only detumble the satellite to the order of magnitude of the orbital rate (10^{-3} rad/s). Since the feedback term is the rate of change in magnetic field, the controller will try to stabilize the satellite about the local magnetic field. This is the cause for the slow rotation of the satellite after detumbling is completed. This is unlike equation (1), which, in theory, can completely stabilize the satellite.

2.2 Selection of Gain

The gain expression, proposed by Avanzini et. al. [1] is based on analysing the closed loop dynamics of the component of angular velocity perpendicular to the earth's magnetic field.

$$k = \frac{4\pi}{T_{orb}} (1 + \sin \xi) J_{min} \quad (4)$$

Here, T_{orb} represents the orbital time of the satellite, ξ represents the inclination of the satellite with respect to the geomagnetic equatorial plane, and J_{min} is the minimum principle moment of inertia for the satellite [2].

3. Hardware

3.1 Sensors

The sensors used during detumbling are magnetometers and an IMU. Magnetometers measure the local magnetic field, whereas the IMU measures angular velocity, as well as the acceleration of the satellite.

3.1.1 Magnetometers

Magnetometers are widely used in satellites as they are relatively small, inexpensive and lightweight. The magnetometers measure a sum of the local magnetic field that is of interest and also the local fields produced by the satellite. The readings could be disturbed due to the presence of magnetorquer coils, ferrous materials on board, and other residual magnetic fields. They have to be calculated and compensated for. As a consequence of this, magnetometer readings are only reliable when there is no current passing through the actuators. Therefore, it must be ensured that there is

no current passing through the magnetorquers while sampling readings from the magnetometer. In addition, the magnetometers must be kept as far away possible from ferromagnetic materials, such as the ferromagnetic core of rod type magnetorquers.

The HMC6343 is selected as the magnetometer for the satellite. It had the primary benefits of being small in size and having a low power requirement of 19.8 mW. In addition, it has the added advantage space heritage, as it has been flown on multiple CubeSat missions. The operating frequencies of the magnetometer are set to either, 1Hz or 10Hz.

3.1.2 Inertial Measurement Unit (IMU)

The inertial measurement unit gives the measure of the external forces and the angular rate of the satellite in body frame. The IMU is a combination of two types of sensors - the 3-axis gyroscopes that measure the angular rate of the satellite and 3-axis accelerometers that measure the acceleration and hence the external forces on the satellite.

The ADIS16334 inertial sensor by Analog Devices was chosen as the IMU for the satellite. Similar to the selection methodology for the magnetometer, this sensor was chosen for its small size, low power consumption relative to its competitors, and space heritage. This sensor consumes a significantly larger amount of power than the magnetometer

3.2 Actuators

Magnetorquers are chosen as actuators during detumbling. This is due to their low power consumption, as compared to alternatives such as reaction wheels. However, this comes at the expense of having an under-actuated system. An in-house magnetorquer system was developed by the team. The design methodology was based upon constraints of mass, power, and size. The torquers must be lightweight and compact enough to be accommodated into the internal architecture of the satellite. They must be powerful enough to detumble the satellite within 3 orbits. In addition, the components of the magnetorquer system must operate within safety guidelines prescribed by the manufacturer. The torque generated by the magnetorquers is represented as follows.

$$\tau = m \times B \quad (5)$$

3.2.1 Magnetorquer Design

Although aluminium is a more lightweight material, copper is chosen as the winding material because it is commercially available at diameters smaller than 1.1 mm. The increase in cross sectional area decreases resistance, thereby increasing power

consumed for a constant voltage supply. Therefore, the use of thinner wires is preferred for minimal power consumption.

For the final configuration, a coil type magnetorquer and a pair of rod-type magnetorquers was chosen. Perm alloy was chosen as a soft ferromagnetic core for the rod-type torquer. Despite having lower power consumption and a smaller mass, a rod type magnetorquer could not be accommodated for the 10cm x 10cm face due to volume constraints. The technical specifications are given in the table below.

Table 1. Magnetorquer Specifications

	Rod Type	Coil Type
Mass (g)	16.91	77.7
Max Power (mW)	72.5	438
Max Moment (Am ²)	0.332	0.324
Winding Material	Awg-39	Awg-30

4. Simulation Methodology

The methodology for simulation of the control laws was based on partitioning the code into sections which can be verified independently. The block diagram given below can help visualize the processes as well as the input-output structure.

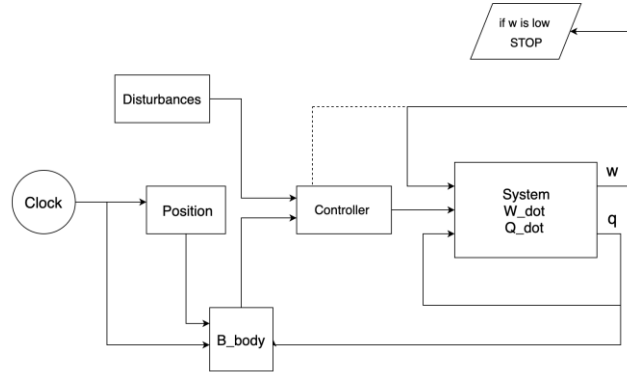


Fig. 1. Block Diagram for Control Law Simulation

4.1 Position Update Module

Using predefined keplerian orbital elements, this module updates the position and velocity of the satellite in ECI frame. The eccentric anomaly is computed iteratively using Newton Raphson's method [3]. In addition, orbital perturbations are accounted for by using the SGP model.

4.2 Magnetic Field Update

The 12th rendition of the International Geomagnetic Reference Field (IGRF) model is used to compute the local magnetic field vector. The output is in the Earth Centered Earth Fixed (ECEF) frame, and

hence, must be converted to the ECI frame with the aid of quaternion multiplication. The transformation between these frames must take into account the revolution of Earth about its spin axis as well as the revolution about the sun. A gaussian error may be implemented in the magnetometer data in order to account for fluctuations in sensor measurement. The amplitude of this noise will correspond to the specifications provided by the sensor manufacturer.

4.3 Controller Module

The inputs to the controller module are the angular velocity and the magnetic field vectors represented in the body frame. For algorithm-2, only magnetic field feedback is required

The component wise magnetic moment is calculated by this module. In addition, the current requirement for the corresponding moment is tabulated in order to keep track of power consumption. If the calculated moment is larger than the limits set by the hardware, then the coil is saturated at the maximum possible value. Errors in the magnetic moment output are may be incorporated as gaussian noise. The error is induced because there might be a disparity between the calculated current and the current supplied by the system.

4.4 State Space Propagation Module

The state variables that are propagated in the simulation are the angular velocity vector, as well as the quaternion which represents rotation between the body and ECI frames. Although the propagation of angular velocity is intrinsic to detumbling, the rotation quaternion should also be propagated in order to simulate the magnetic field vector in the body frame. This component is critical in computing the necessary control torque. The non-linear state equations are represented below.

$$\frac{d\omega}{dt} = I^{-1}(-\omega \times (I\omega) + \tau_{con} + \tau_{dis}) \quad (6)$$

$$\frac{dq}{dt} = \frac{1}{2}\Omega(\omega)q \quad (7)$$

$$\Omega(\omega) = \begin{bmatrix} 0 & \omega_3 & -\omega_2 & \omega_1 \\ -\omega_3 & 0 & \omega_1 & \omega_2 \\ \omega_2 & -\omega_1 & 0 & \omega_3 \\ -\omega_1 & -\omega_2 & -\omega_3 & 0 \end{bmatrix} \quad (8)$$

Here, I represents the inertia tensor of the satellite, τ_{con} is the control torque calculated using (4) , and τ_{dis} represents the disturbance torques.

Propagation is carried out by using a fourth order Runge Kutta (RK4) numerical integration. The iterative scheme is presented as follows.

$$\omega_{t+1} = \omega_t + \frac{1}{6}(k_{w1} + 2k_{w2} + 2k_{w3} + k_{w4})\Delta t \quad (9)$$

$$q_{t+1} = q_t + \frac{1}{6}(k_{q1} + 2k_{q2} + 2k_{q3} + k_{q4})\Delta t \quad (10)$$

$$k_{\omega i} = \left. \frac{d\omega}{dt} \right|_{\omega(i)}, \omega_i = \omega_o + ak_{\omega(i-1)}\Delta t \quad (11)$$

$$k_{q i} = \left. \frac{dq}{dt} \right|_{q(i),w(i)}, q_i = q_o + ak_{q(i-1)}\Delta t \quad (12)$$

$$a = \begin{cases} 0 & i = 1 \\ 0.5 & i = 2, 3 \\ 1 & i = 4 \end{cases} \quad (13)$$

In this scheme the quaternion is normalized at after every calculation of k_{q_i} in order to maintain unit magnitude. The magnetic field vector is also recalculated in each step so as to simulate the change in ambient magnetic field the perspective of the body frame. This results in the torque acting on the body changing as the magnetic field rotates. This is a reflection of the fact that the torque produced will attempt to align the magnetic dipole with the local magnetic field. Therefore, a closer representation of space environment is achieved.

Initially simulations were performed using Euler's method due to ease of implementation. However, the tabulated ordinary differential equations are highly sensitive and non-linear, and hence, required a much lower time step as compared to the time step required in the RK4 method in order to achieve convergence. The lower time step led to a much higher computation time despite using a simpler numerical method. Therefore, it is recommended that a higher order integration scheme should be employed for propagating satellite dynamics.

4.5 Disturbance Module

Disturbances are introduced into the simulation in order to verify the robustness of the controller under the influence of perturbations. Within the space environment the satellite experiences disturbance torques due to aerodynamic drag, gravity gradient, solar radiation pressure, and residual magnetic moments. Two approaches were undertaken to simulate disturbances.

3.5.1 First Approach

A calculation of the maximum disturbance torque for each category of external disturbance forces was tabulated. The magnitude of maximum possible disturbance torque acting on the satellite will be the sum of the individual magnitudes. Note that an added margin of 30% was included to this value. Now, a random unit vector is generated, and thereby, a torque of maximum possible magnitude is generated along this direction. This disturbance torque is added to the satellite dynamics.

However, although this method introduces a high degree of disturbance in the system, it doesn't have an intuitive basis. It is probable for a given trial run, that a majority of the disturbance torques generated are anti-parallel to the direction of angular velocity, and hence, aiding the detumbling progress. A remedy to overcome such cases is to run this simulation multiple times under a different set of disturbances and find an average of the settling time.

3.5.2 Second Approach

Since the aerodynamic drag is by far the maximum source of disturbance force for the satellite and acts opposite to the direction of velocity, a disturbance force vector is generated antiparallel to the direction of velocity. Its magnitude will be the sum of the maximum magnitude of disturbance force possible within each category. This disturbance force is then transformed under rotation and represented in the body frame. The torque produced by this force will act perpendicular to the vector between the centre of pressure and the centre of mass of the satellite. This method of adding disturbances may not provide maximum possible perturbations to the satellite, but it better represents the actual dynamics of the satellite.

5. Results and Discussion

The detumbling algorithms were tested with the parameters listed in Table 2. Worst case angular velocity is reported as 10 degrees per axis [4]. A margin of 50 percent per axis is taken to ensure robustness. It is assumed that at the start of the simulation, the ECI and ECEF frames are aligned. Orbital parameters are selected for a sun-synchronous, LEO orbit with an altitude of approximately 600 km. The simulation terminated when the angular velocity on

all three axes was less than or equal to twice the orbital rate.

Table 2. Orbital Parameters

Parameter	Value
Inclination (deg)	97.8
Altitude (km)	607
Eccentricity	7.15×10^{-5}
Initial Angular Velocity	$(.03, -.03, .03)^T$

Both algorithms were tested using the first approach for disturbances over 1000 runs for the same right ascension and argument of perigee. For the second approach for disturbances, the right ascension was varied over 10 different values varying by 36 degrees since it will affect the spatial change in the IGRF model. The detumbling time for algorithm 1 was less than the Bdot algorithm in all runs. The disparity in detumbling time was approximately equal to half of the orbital rate. In addition, the magnetorquers weren't saturated at any instant for either case. This indicates that the torquer design is powerful enough for the system?

When comparing the reduction of angular velocity component wise, the z-component of angular velocity requires the most time because the magnitude of magnetic field driving the detumbling process is lower compared to the x and y components. Component wise response to detumbling control is given below for a test run using the Bdot algorithm.

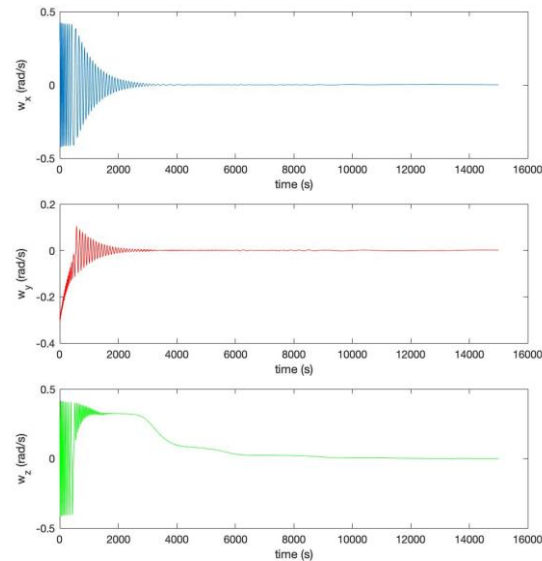


Fig 2. Component-wise Angular Velocity vs Time

6. Conclusions

The settling time of the controller for algorithm 1 was smaller than the Bdot controller for all nominal cases. However, the difference in detumbling time of the two algorithms was not significant as per the requirements of the satellite. Bdot has the added advantage of consuming less power as it does not use the IMU for angular velocity feedback. The IMU, used in algorithm 1 consumes a significant amount of power. The energy expenditure of the IMU outweighs the advantage of having a smaller detumbling time. Hence, based on our analysis and simulation, the Bdot control law was selected as a more efficient detumbling algorithm for a 3U CubeSat. In order to verify if the satellite is detumbled, the IMU will be used at sparse intervals. In cases where the angular velocity exceeds a critical amount (>100 deg/s), the detumbling mode will not be initiated and the satellite will detumble naturally.

7. Future Work

By using the results from the simulation, the Team is moving towards hardware in the loop testing (HIL). This includes the fabrication and testing of the magnetorquers. This will be done with the aid of a Helmholtz cage [6] in order to monitor and regulate the magnetic field of the environment. Here, we can verify the amount of residual magnetization present in the ferromagnetic rod. In addition, the team is working on the accurate determination of Bdot from magnetometer data which may require the implementation of a low pass filter to remove unwanted noise.

Acknowledgements

The authors would like to thank the following:

1. Team Anant, the Student Satellite Team of BITS Pilani for providing the motivation to carryout these simulations.
2. Dr. Kaushar Vaidya, Rudrakh Panigarhi, and Jeet Yadav for their constant support and technical expertise in perusing research for this paper.
3. The administration of BITS Pilani and Indian Space Research Organization (ISRO) for giving us an opportunity to work on building a satellite.

References

- [1] Giulio Avanzini and Fabrizio Giuliotti, "Magnetic Detumbling of a Rigid Spacecraft", JOURNAL OF GUIDANCE, CONTROL, AND DYNAMICS, Vol. 35, No. 4, July–August 2012
- [2] F. Markley and J. Crassidis, Fundamentals of spacecraft attitude determination and control, New York: Springer, 2014.
- [3] Oliver Montenbruck and Eberhard Gill, Satellite Orbits, Springer, 2005.
- [4] Mr. Rutwik Narendra Jain, et. al., "Modes of Operation for a 3U CubeSat with Hyperspectral Imaging Payload", 69th International Astronautical Congress, 2018.
- [5] Goyal, Tushar & Aggarwal, Kushagra. (2019). Simulator for Functional Verification and Validation of a Nanosatellite. 1-8. 10.1109/AERO.2019.8741886.
- [6] Goyal, Tushar. (2017). Design and Development of a Three-Axis Controlled Helmholtz cage as an In-House Magnetic Field Simulator for CubeSats.